IEEE Access
Multidisciplinary ⋮ Rapid Review ⋮ Open Access Journal

Received 29 November 2022, accepted 6 January 2023, date of publication 12 January 2023, date of current version 18 January 2023.

Digital Object Identifier 10.1109/ACCESS.2023.3236403

RESEARCH ARTICLE

Distributed Energy-Efficient Clustering and Routing for Wearable IoT Enabled Wireless Body Area Networks

MUHAMMAD YEASIR ARAFAT[1], SUNGBUM PAN[2], (Member, IEEE), AND EUNSANG BAK[2]
[1]Department of Computer Engineering, Chosun University, Gwangju 61452, Republic of Korea
[2]IT Research Institute, Chosun University, Gwangju 61452, Republic of Korea

Corresponding author: Eunsang Bak (bakeunsang@chosun.ac.kr)

This work was supported by the Basic Science Research Program through the National Research Foundation of Korea (NRF) funded by the Ministry of Education under Grant 2017R1A6A1A03015496.

ABSTRACT Recently, the wearable internet of things (WIoT) has brought a new dimension of connectivity to wireless body area networks (WBANs). For instance, the WIoT provides valuable functions, such as collecting, analyzing, and transmitting data for real-time health monitoring of medical services. However, designing a clustering and routing protocol is challenging because WIoT attributes are subject to high interference in dense deployment, social mobility, and limited energy. In a WIoT-enabled WBAN, cooperative control is the fundamental function of clustering and routing. Cluster-based routing protocols are preferred for WBAN because of their scalability. However, one-hop neighbor-based clustering approaches do not ensure connectivity and reachability owing to node mobility. The existing two-hop-based clustering protocols are mostly centralized-based approaches, which are unsuitable for dynamic WBANs. In this paper, we propose a distributed energy-efficient two-hop-based clustering and routing protocol (DECR) targeting WIoT-enabled WBAN. In DECR, in the cluster formation phase, each node obtains the information of its neighbor nodes within the two-hop range. We utilize the modified grey-wolf optimization algorithm for the cluster head (CH) selection and routing optimization. Node connectivity and residual energy were jointly considered when determining the CH in each cluster. We also developed an analytical model to determine the optimal number of clusters by considering intra- and inter-cluster transmission distances to reduce the overall transmission distance and number of transmissions. Finally, we proposed a routing algorithm to ensure energy-efficient packet delivery from CH to sink. Our simulation outcomes revealed that the proposed DECR significantly outperforms the existing clustering and routing protocols in various performance metrics.

INDEX TERMS Wearable internet of things, clustering, two-hop range, distributed, cluster head, energy-efficiency, grey wolf optimization, routing, wireless body area network (WBAN).

I. INTRODUCTION

Recently, the wearable internet of things (WIoT) has fascinated increased interest in both academic and industrial areas because of its wide range of potential applications. WIoT enables a new dimension of wireless connectivity in wireless body area networks (WBANs), which helps improve the remote healthcare system and real-time health monitoring [1]. According to the Statistics Korea report, 16.5 percent of South Korean population was aged 65 and older in 2021, which, by 2050, will be more than 44 percent [2]. Due to the large number of aged people, the cost of healthcare may increase significantly. In this case, WBANs can provide senior citizens with a cost-effective healthcare system [3]. WBANs can be a possible solution for the aging society's healthcare, various chronic diseases, and shortage of medical facilities. Owing to the advancement of microprocessors, Wi-Fi interfaces, global positioning systems (GPS), wireless charging, battery technology, smart watch, smartphones, wearable technology, unmanned aerial vehicles, and

The associate editor coordinating the review of this manuscript and approving it for publication was Adamu Murtala Zungeru.

various sensors, modern healthcare systems have widely used WBANs [4].

WBANs can be categorized into three tiers of level communication: Intra-WBAN, inter-WBAN, and beyond-WBAN communications [5]. Tier-1 is intra-WBAN communication, consisting of a set of sensors placed on or implanted into the human body. Tier-2 is inter-WBAN communication using smartwatches, smartphones, and personal computers. Ad hoc architecture is distributed to communicate in this tier with a random topology. The function of Tier-2 is to forward the information sent by the sensor to Tier-3 (terminal center) through 3G/4G/5G, WLAN, and other wireless technologies.

In recent years, wearable devices are becoming a potential candidate for the hub of IoT and WBANs [6]. Wearable devices have become famous for health monitoring tools since they can collect data from human body biosensors and transmit vital data while moving [7]. Wearable devices enhance the quality of human life and make our daily life safe. WBAN can be realized in an ad-hoc manner consisting of WIoT devices. Due to the significant increase in WIoT users, we predict that within the next few years, the number of WIoT users and mobile phone users will be the same [8]. In addition, the densely deployed WIoT may cause interference between adjacent WBANs. Therefore, the interference between inter-WBANs should be eliminated to maintain the quality of the network. Besides the characteristics of traditional wireless sensor networks (WSNs), such as limited battery capacity, low computational power, and unreliable wireless channel, WIoT-based WBANs have many unique features, including highly dynamic network topology, time-varying channel quality, and high mobility [9].

Moreover, to maintain reliable data communication, cluster-based routing protocols are widely used in existing literature [10]. One of the main challenges associated with WBANs is the reliable transmission of data to a sink while minimizing the power consumption of the WBAN [11]. In WBANs, clustering is utilized to maintain the topology of networks, and routing establishes the path between the source to the destination node for reliable data transmission. Since WIoT devices generally have limited battery capacity, WBAN lifetime is determined by the energy consumption rate of WIoTs. Thus, energy efficiency is a key issue in designing the clustering and routing protocol in WBANs. There are two well-known approaches for clustering; one is centralized, and another is distributed. Centralized clustering is suitable for small and static networks. However, for dynamic networks, distributed clustering is widely used in existing literature [12]. Moreover, the dual sink approach is more reliable in WBANs in terms of network lifetime, network stability, and energy efficiency [13].

To reduce energy consumption in WBANs, researchers have come up with various new ideas. Energy-efficient clustering and routing are key research issues [14]. Generally, in the cluster-based approach, the entire network is divided into several groups or clusters, where the network follows a hierarchical structure. Most clustering approaches divide all nodes into two categories: Cluster member (CM) and cluster head (CH). A CH is elected among all nodes in the cluster based on node positions, energy, and the degree of a node. CMs sense and collect the data, then transmit them to the CH; the CH node is responsible for transmitting the data to the sink node. The clustering approach solves the network topology control and long-distance communication issues. Therefore, cluster-based routing protocols reduce the node energy consumption, prolong the network lifetime, and have a low communication overhead. Due to human social mobility, WIoTs move at random. Hence, network topology control becomes an important issue, which makes the proposed cluster distributed and self-organized. Moreover, intra- and inter-cluster distance affect the optimization of clustering. Therefore, the minimization and maximization of these parameters make topology control an NP-hard problem.

Recently, several meta-heuristic algorithms have been widely used to find optimal solutions for NP-hard problems [15]. Meta-heuristic algorithms have become popular among researchers due to their flexibility, simplicity, and low complexity. For example, over the past two decades, several bio-inspired optimization methods such as particle swarm optimization [16], grey-wolf optimization [17], and whale optimization [18] have been widely used in different kinds of ad-hoc networks for localization, topology control, clustering, CH selection, and routing.

However, system complexity and overhead may increase by considering two-hop neighbor information [19]. At the same time, two-hop neighbor information extends the local view of the network. The availability of more information about the network topology increases the overall network performance. In the existing literature [20] and [21], it is observed that the clustering and routing protocol based on two-hop neighbors provides stable clustering and requires a smaller number of hops from source to destination compared with one-hop neighbors information-based clustering and routing. However, due to the significant increase in system complexity and overhead, considering three- or more-hop neighbors is less attractive for clustering and routing. Thus, choosing two-hop neighbor is the tradeoff between performance enhancement and protocol complexity.

A. CONTRIBUTION OF THE STUDY

This article proposes a distributed energy-efficient clustering and routing protocol (DECR) for WIoT-enabled WBAN. For the clustering purpose, we utilized two-hop neighbor information. Two-hop neighbor information extends the local view of network topology, which assists in handling the node mobility and network topology change. The primary contribution of the article is summarized as follows:

- In the clustering phase, to optimize the cluster intra- and inter-transmission distance, we utilized two-hop neighbor information for cluster formation. Moreover, two-hop neighbor information extends the local view of network topology, which assists in making optimal

routing decisions. An optimal energy-efficient clustering prolongs the network lifetime by reducing the network energy consumption.

- In the CH selection phase, we utilized a modified grey-wolf optimization (MGWO) algorithm to select the CH node. For energy-efficient transmission in intra-cluster communication, the CH plays a key role. In our proposed approach, a distributed intra-cluster routing is performed based on a one-hop neighbor node as a relay for transmitting data to the CH in the two-hop neighbor-based cluster. MGWO utilized the WIoT node fitness value to select the CH. MGWO optimizes the average transmission distance among the nodes within the same cluster.
- In the routing phase, CH utilized MGWO-based routing to transmit the data to the sink node via the CH. The proposed approach utilized the grey-wolf hierarchical structure to transmit data, which minimizes long transmissions and reduces the transmission distance to each CH.

B. OUTLINE OF THE PAPER

The remainder of this paper is arranged in the following way. Section II shows a brief overview of existing literature in this field. In Section III, we examined the preliminaries concerning the motivating scenario, network model, and energy model. Section IV presents the proposed DECR algorithms, including cluster formation, CH selection, and routing. An extensive computer simulation is conducted to evaluate the performance of DECR, compared with the existing approaches in terms of various performance metrics. Finally, in section VI, we present conclusions and future works.

II. REVIEW OF RELATED STUDIES

Due to the recent development in wireless communication and IoT devices, WBAN has become the new dimension of the remote healthcare system. WBAN works in a three-layer architecture. The tire-1 consists of various body sensors. These body sensors collect biosignals from the human body and transmit them to a body control unit, for instance, PDA. In wireless communication, the tire-1 is classified as an intra-WBAN communication, where sensor nodes are static, and the distance between sensor nodes and PDA is very short. The tier-2 forms a network of WBANs composed of several intra-WBANs. Moreover, the tier-2 WBAN contains inter-WBAN communication, where biosignals are further transmitted to the sink node in a multi-hop communication fashion. In modern times, many IoT devices, such as smart watches, WIoT, smart clothing, activity tracker, smart footwear, medical wearable, patches, and jewelry [7], work as tier-2 communication. The Tier-3 network supports emergency services, hospital networks, doctors, medical workers, and emergency transports. In the last decade, much research has been done on intra-WBAN communication. Due to the recent development of WIoT, now is the time to focus on inter-WBAN communication in an ad hoc manner. Several research works have been done for inter-WABN communication. However, there have been many unsolved issues such as social mobility issues, energy consumption, network lifetime, and reliability of communication systems.

Mu et al. [3] presented a spectrum allocation method for inter-WBAN. The approach tried to mitigate the inter-WBAN interference in a dense deployment using a machine learning-based intelligent partition method for clustering. They considered human social mobility for topology control and clustering. The simulation result shows that the proposed approach performs well in the fast topology of altering inter-WBAN. Mu et al. [22] presented a self-organized dynamic clustering (SDC) method to minimize the interference between multiple WBANs. The proposed method borrowed the cellular network concept to allocate the channel between multiple WBANs. The self-organized method enhanced the reliability of data transmission between inter-WBAN. They used frequency division multiple access (FDMA) and time division multiple access (TDMA), where FDMA works with a cluster framework and TDMA operates on a superframe structure. In [23], the authors proposed a co-channel inter-WBAN coexistence method empowered by a bio-inspired model to avoid inter-WBAN interference. Each WBNA sends a superframe in a distributed manner to avoid interference. Cellular-assisted D2D communication with a radio resource allocation scheme is used to minimize the collision between two WBANs when they are within the radio range of each other [24].

Shimly et al. [25] investigated the cross-layer routing performance for inter-WBAN. In this research, they analyzed the performance of shortest-path routing (SPR) and cooperative multi-path routing (CMR). The performance shows that the alternative paths in CMR performed well in terms of throughput, end-to-end delay, and energy consumption. Zahid et al. [26] proposed an energy-efficient harvested-aware clustering and cooperative routing called E-HARP. The main contributions of the E-HARP are dynamic CH selection and cooperative routing. First of all, an optimal cluster is selected based on the cost function. A cost function is designed based on node residual energy, required transmission power, link signal-to-noise ratio (SNR), and energy loss. Secondly, a routing protocol applies through the CM nodes' cooperative effort. The performance shows that E-HARP performed well in energy consumption, throughput, delay, and network lifetime. Olivia et al. [27] proposed a data-centric load-aware routing protocol called DLQoS for dynamic WBAN to address the network congestion and prolong the network lifetime. In this protocol, they considered data delivery time, reliability, throughput, and network lifetime as key data-centric parameters. To ensure the performance of data-centric paraments, they jointly considered the neighbor nodes' link quality and node information. Moreover, the proposed protocol distributed the traffic load by a buffer management system since node mobility significantly impacts

clustering and routing protocol performance, resulting in frequent topology changes and packet loss. Asim et al. [28] proposed an efficient cluster formation for IoT-enabled WBAN called MT-MAC. To ensure network integrity, the authors considered the node handover mechanism among the virtual clusters in the network. Simulation results reveal that MT-MAC reduces significant packet loss during node mobility.

Li et al. [29] investigated the performance analysis for body-to-body networks (BBNs), where an end-to-end delay and packet loss are key performance metrics. In this research, all nodes can freely and stochastically move in the network area. Taking into account node mobility, they introduced node entrance probability and network entrance probability in the proposed framework. Moreover, they used the Markov chain model for node behaviors. Simulation shows the effectiveness of the proposed approach for mobile WBAN. Raj et al. [30] proposed an opportunistic energy-efficient and load balance-aware routing protocol for WIoT-enabled WBAN. The authors address the WIoT data aggression delay and routing loops in the proposed protocol. Fawad et al. [31] proposed a clustering and routing technique based on ant lion optimization (ALO) for WBAN. They utilized the ALO algorithm for the optimal number of clusters. The result shows the effectiveness of the ALO algorithm compared to existing other bio-inspired algorithms in various scenarios. Khan et al. [32] proposed energy-harvested and cooperative-enabled energy-efficient routing called EHCRP for IoT-WBANs. They considered multiple parameters for path cost calculation, such as node residual energy, number of hops from source to sink, traffic congestion, path quality, and available bandwidth. Due to the path cost estimation function, EHCRP performs well during data transmission by multi-hop routing. According to [33], a dynamic hierarchical protocol based on combinatorial optimization (DHCO) is proposed to achieve a balance between sensor node energy consumption and network longevity. Instead of selecting the cluster head or the next hop node, the DHCO algorithm establishes a feasible routing set for each sensor node. Authors in [34] provide an overview of various multi-objective optimization algorithms. Towards improving the energy efficiency of ultra-dense WSNs, the authors proposed the use of a combined approach of unsupervised learning and genetic algorithms [35]. A novel algorithm was proposed in [36] that applies machine learning techniques and genetic algorithms to improve the performance of ultra-reliable and low-latency WSNs (uRLLWSNs). In the proposed algorithm, the fetal dataset, denoted by the population, is designed by utilizing the K-means clustering algorithm to construct a two-tier network topology. A method for energy conversion is then developed to prevent cluster heads from becoming overloaded during clustering. The purpose of this multi-objective optimization model is to simultaneously address multiple optimization objectives including the maximum network connectivity and reliability as well as the longest network lifetime. Table 1 summarizes the clustering and routing protocols in WBANs.

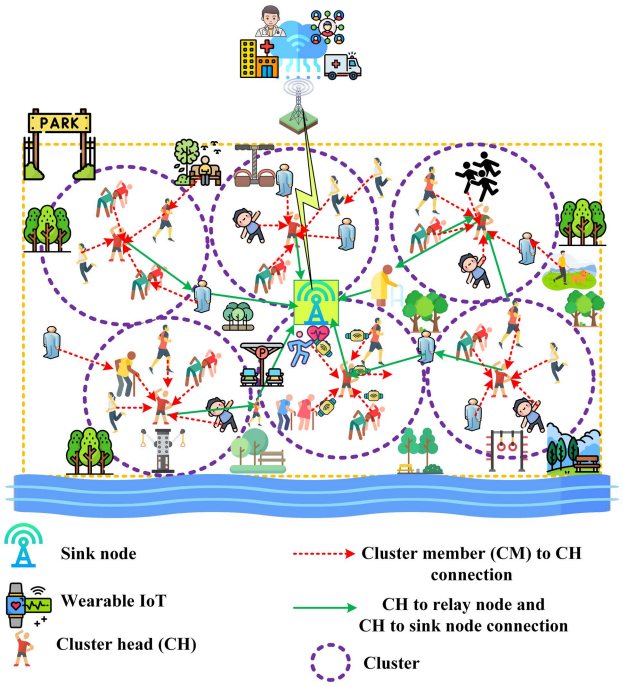

FIGURE 1. WIoT-enabled WBAN: WIoT users are organized into clusters. Cluster members are transferred data to the sink using multi-hop routing.

III. PRELIMINARIES

In this section, we introduce a motivational scenario, network model, assumptions, energy model, and the associated assumptions. In addition, the MGWO algorithm is explained as preliminary knowledge of our study. Here are the notations used throughout the paper in Table 2.

A. MOTIVATION SCENARIO

In this paper, we consider the application of WBAN in a public space such as a park or outdoor exercise area. In the scenario, all users have WIoT devices such as a smartwatch. A smartwatch collects the body biosignal from the various sensors installed in the human body. The received biosignal from the human body is transmitted to a static sink node in the deployed area, as shown in Fig. 1. In our application scenario, we assumed that the position of the sink node is in the middle of the deployed area. In addition, the sink node has a 5G module to transmit the data to the healthcare monitoring center for further processing. In this model, we demonstrated that users transmit the WIoT-sensed data to the sink node by multi-hop communication.

B. SYSTEM MODEL AND ASSUMPTIONS

In our network model, we considered n number of WIoT devices that are uniformly distributed and randomly deployed in a $M \times M$ square region, and the sink node is placed at the center of the region, as shown in Fig. 1. Moreover, all the WIoT users have human walk mobility at a speed of 2–5 m/s [37]. All the WIoT nodes have a communication radius of R, which is a circular area. Initially, all WIoT nodes

TABLE 1. Summary of clustering and routing protocols in WBANs.

Protocol	Architecture	Structure	Factor of CH selection	Advantages	Limitations
SDC [22]	Distributed	Cluster-based and single-hop	N/A	Self-organized clustering	Lack of analysis of CH selection process
E-HARP [26]	Centralized	Cluster-based and single-hop	Residual energy, transmission power, and link quality	Utilized energy harvested technique	Not suitable for Inter-WBAN communication
DLQoS [27]	Centralized	Flat-based and multi-hop	N/A	Delay efficient protocol	Control overhead may increase in large-scale WBAN
MT-MAC [28]	Distributed	Cluster-based and multi-hop	N/A	User mobility-aware clustering method	Lack of analysis of mobility effect on network topology change
BBNs [29]	Distributed	Flat-based and multi-hop	N/A	Low network latency	Higher protocol complexity
ALOC [31]	Distributed	Cluster-based and single-hop	N/A	Minimize the number of transmissions	Network topology change may reduce the cluster lifetime
EHCRP [32]	Distributed	Flat-based and multi-hop	N/A	Energy-efficient approach	Routing overhead may affect the protocol performance
DHCO [33]	Distributed	Hierarchical and multi-hop	N/A	Increase network lifetime	Applicable for WSN
uRLLWSNs [36]	Distributed	Cluster-based and multi-hop	N/A	Low latency approach	Applicable for static large-scale WSN

TABLE 2. Notations.

Notation	Description
$N_n(i)$	the set of n-hop neighbor nodes of the node i.
	$N_{1-m}(i)$: $N_1(i) \cup N_2(i) \cup \cdots \cup N_m(i)$
	$N_1(i) = N(i)$
$E^{re}(i)$	the residual energy of the node i.
$E^{int}(i)$	the initial energy of the node i.
$E_{\text{Tx}}(l, d)$	the energy for transmitting l bits of data over d distance.
$E^{re}_{N_n}(i)$	the set of residual energies of N_n of the node i.
$E_{\text{Tx}(A,B)}$	the energy for transmitting data between A and B.
$E_{\text{Rx}(A,B)}$	the energy for receiving data between A and B.
$d(\text{CH}, n\text{h})$	the average distance between a CH and its N_n nodes.
$d(n\text{h}, m\text{h})$	the average distance between N_n and N_m nodes.
t_{max}	the maximum number of iterations
E_{total}	the total energy consumption of the entire network
C_{opt}	the optimal number of clusters
CH_m	The m-*th* number of CH
RP	the routing path
F	the fitness function
TCR_i	two-hop connectivity ratio of node i.
EF_i	energy factor of node i.
NSF_i	stability factor of node i.

have the same energy level and are aware of it. There is no further energy supply when all the WIoT nodes are deployed.

When a node drains off its battery power completely, it is considered a dead node. Each node can measure the distance between its neighbor nodes, or the sink node based on the received signal strength indicator (RSSI). The sink node has unlimited energy, processing power, and buffer capacity and can cover the entire deployed area. The proposed DECR has three phases: clustering, CH selection, and routing, as shown in Fig. 2. In the next section, we explain all three phases.

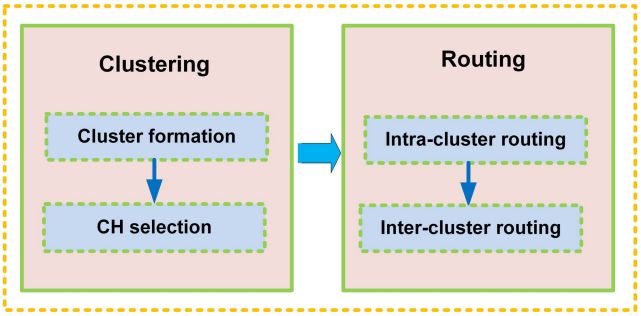

FIGURE 2. Block diagram of the DECR framework.

C. ENERGY MODEL

In this paper, we utilized the first-order radio model [16] to measure the energy consumption of the WIoT nodes. The required energy for transmitting l bits of data over d distance is $E_{Tx}(l, d)$, and the receiving energy is $E_{Rx}(l)$. The equations of transmitting and receiving energy are represented by Equations 1 and 2, respectively.

$$E_{\text{Tx}}(l, d) = \begin{cases} l \cdot E_{\text{elec}} + l \cdot \varepsilon_{f_s} \cdot d^2, & \text{if } d < d_0 \\ l \cdot E_{\text{elec}} + l \cdot \varepsilon_{mp} \cdot d^4, & \text{if } d \geq d_0, \end{cases} \tag{1}$$

$$E_{\text{Rx}}(l) = l \cdot E_{\text{elec}}, \tag{2}$$

where E_{elec} is the energy required for electronic circuitry, d_0 is the threshold distance, and εf_s and ε_{mp} are the energy associated with the transmitter amplifier for free-space fading and multipath fading respectively. Threshold distance can be calculated as follow

$$d_0 = \sqrt{\frac{\varepsilon_{f_s}}{\varepsilon_{mp}}}, \tag{3}$$

D. MGWO ALGORITHM

MGWO is inherited from the GWO algorithm. The GWO is one of the bio-inspired optimization algorithms designed based on grey wolves' leadership and hunting strategy [38]. The main principle of the GWO algorithm is simplicity. Hence, a quick speed and high–precision search is easy to achieve using this model. GWO is widely used to solve many optimization problems in the real world. Several swarm algorithms mimic the hunting and searching behaviors of some animals. For example, in GWO, wolves are labeled into four categories: alpha (α), beta (β), delta (δ), and omega (ω). The alpha wolf is the dominant leader and decision-maker. The beta wolf helps the alpha wolf to make decisions, and the beta takes over the alpha if the alpha passes away. The delta wolf is the third strong wolf who dominates the omega wolf, and the omega wolf follows the orders of the alpha and beta wolves. As the GWO algorithm follows the leadership hierarchy between wolves, three solutions can be obtained during the optimization process. Therefore, compared to other bio-inspired algorithms, the GWO has significantly less probability of yielding premature solutions or falling into a local minimum [39] and [40].

The grey wolf hunting behavior follows three steps: finding, encircling, and attacking the prey. The population of N wolves is denoted as $\mathrm{X} = [X_1, \ldots, X_n, \ldots, X_N]$. Position of the nth wolf in D dimensional search space is defined as $X_n = \left[X_n^1, \ldots, X_n^d, \ldots, X_N^D\right]^T$. The mathematical model for grey wolf hunting [41] behavior can be represented as

$$X_n^d(t+1) = X_p^d(t) - A_n^d \left| C_n^d \cdot X_p^d(t) - X_n^d(t) \right|, \quad (4)$$

where t is the iteration, X_p^d is the position of the prey in d dimension, and $A_n^d \left| C_n^d \cdot X_p^d(t) - X_n^d(t) \right|$ is the size of the encirclement. A_n^d and C_n^d are coefficient vectors denoted by

$$A_n^d = 2a \cdot r_1 - a, \quad (5)$$

and

$$C_n^d = 2 \cdot r_2, \quad (6)$$

where r_1 and r_2 are random numbers between [0, 1], and variables a (decreasing linearly from 2 to 0) are the functions of the iteration steps:

$$a = 2\left(1 - \frac{t}{t_{max}}\right), \quad (7)$$

where t shows the current iteration and t_{max} is the maximum number of iterations [42].

To find the optimal solution, the GWO algorithm simulates the behavior of wolves. It utilized three fittest solutions and, in turn, used these three solutions to update other solutions. For other iterations, the positions of the wolves are updated as follows:

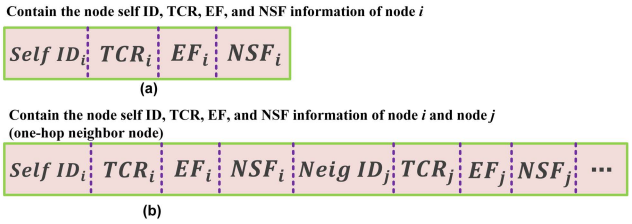

FIGURE 3. Hello packet format.

$$X_{n,\alpha}^d(t+1) = X_\alpha^d(t) - A_{n,\alpha}^d \left| C_{n,\alpha}^d \cdot X_\alpha^d(t) - X_n^d(t) \right|, \quad (8)$$

$$X_{n,\beta}^d(t+1) = X_\beta^d(t) - A_{n,\beta}^d \left| C_{n,\beta}^d \cdot X_\beta^d(t) - X_n^d(t) \right|, \quad (9)$$

$$X_{n,\delta}^d(t+1) = X_\delta^d(t) - A_{n,\delta}^d \left| C_{n,\delta}^d \cdot X_\delta^d(t) - X_n^d(t) \right|, \quad (10)$$

$$X_n^d(t+1) = \frac{1}{k} \sum_{k \in \alpha,\beta,\delta} X_{n,k}^d(t+1) \quad (11)$$

where k denotes the three wolves α, β, and δ, and $k = 3$.

The standard GWO algorithm only considers the global best value without considering individual wolf experiences during iteration. To consider the individual wolf experience, we added the memory in each wolf inspired by the PSO algorithm. Finally, the proposed MGWO updates the positions as follows:

$$X_n^d(t+1) = \mu_1 \cdot \frac{1}{k} \sum_{k \in \alpha,\beta,\delta} X_{n,k}^d(t+1) + \mu_2 \cdot r_3 \cdot \frac{1}{k} \sum_{k \in \alpha,\beta,\delta} \left(X_{n,best}^d - X_{n,k}^d(t)\right), \quad (12)$$

where social and individual learning factors of wolves are defined by μ_1 and μ_2 respectively, r_3 is a random value with range [0, 1], and $X_{n,best}^d$ represents the personal historical best solution of the wolf.

IV. DECR ALGORITHMS

In this section, the DECR algorithms for WBANs are discussed in detail, which include clustering, CH selection, and routing algorithm.

A. TWO-HOP NEIGHBOR DISCOVERY

For the two-hop clustering in a distributed fashion, each node needs to obtain its two-hop range neighbor information.

Hello packet is used to obtain the neighbor node information in our case node two-hop connectivity ratio (TCR), energy factor (EF), and node stability factor (NSF). The node EF indicates residual energy level. Each WIoT node has its immediate one-hop and two-hop neighbor nodes. Moreover, each node has its unique identification number and has a neighbor table containing various neighbor information in the Hello packet formulated in Fig. 3.

Any node i needs to broadcast the initial Hello packet, as shown in Fig. 3(a), before a new round starts. The Hello

TABLE 3. Simulation parameters.

Parameter	Value
Simulator	MATLAB
Target area	Scenario-1: 100 m × 100 m Scenario-2: 200 m × 200 m
Number of nodes	50–200
Number of sinks	1
Position of the sink	Scenario-1: (50, 50) Scenario-2: (0, 0)
Node speed	2–4 m/s
Mobility model	RWM
Initial energy of node	2 J
Transmitter/ receiver electronics E_{elec}	50 nJ/bit
ε_{fs}	10 pJ/bit/m^2
ε_{mp}	0.0013 pJ/bit/m^4
Packet size	4000 bits
Data aggregation energy cost	50 nJ/bit
MAC protocol	Bluetooth 5.0
Sensing range	50–120 m
Frequency	2.4 GHz
Bandwidth	20 MHz
Antenna	Omni-directional
Propagation model	Free-space
Traffic type	CBR
CBR rate	2 Mbps
Transport protocol	UDP
Number of iterations t_{max}	150
Total simulation time	1000 s
Compared routing protocols	MT-MAC and ALOC

packet contains $SelfID_i$, TCR_i, EF_i, and NSF_i. If a node i receives the Hello packet from a node j, it indicates the node i and j are within a one-hop communication range (R). In the same way, the node j exchanges the Hello packet with the node i. After that, the node i updates its neighbor tables, which contain the node j information, as shown in Fig. 3(b). The neighbor table contains valuable information about neighbor nodes including node position, energy level, and distance. In this way, the node i obtains the one-hop neighbor information from the node j. However, the node i detects the node k information from the node j Hello packet, which indicates that the node k does not have direct communication with the node i, and the node k is a two-hop neighbor node of the node i. Through this process, we obtain the one-hop and two-hop neighbor node information.

B. TCR

To extend the local view of the network we utilized TCR [43], which presents the connectivity ratio of a node with its neighborhood. To obtain the TCR, a node accesses its two-hop neighbor node information. The TCR value for a node i is calculated as follows:

$$\psi_i = \frac{\left[\sum_{j\in N_2(i)}^{N_2(i)} \frac{|N(j)|}{j\in N_2(i)}\right] + |N(i)|}{[N_2(i)]+1}, \tag{13}$$

$$TCR_i = |N(i)| - \psi_i, \tag{14}$$

where $N_2(i)$ is the two-hop neighbor nodes of the node i and ψ_i is the average connectivity within the two-hop neighbor node of the node i. A node having a high TCR value indicates that it has a large number of neighbor nodes within its transmission range. Such a node is considered to be selected as a CH node.

C. EF

As we mentioned earlier, initially all the nodes have the same energy level. However, after several rounds, the battery starts to drain. Nodes placed near the sink node and CH nodes drain the battery faster than other nodes because of further processing and communication tasks. Therefore, the node residual energy is critical in extending the network lifetime by choosing a CH node considering energy balance. The residual energy level of node i can be calculated as follows:

$$EF_i = \frac{E^{re}(i)}{E^{int}(i)}, \tag{15}$$

where $E^{re}(i)$ and $E^{int}(i)$ are the residual and initial energy of node i, respectively. As we consider the two-hop neighbor range, the normalized energy factor for the two-hop range can be estimated as follows:

$$\phi_i = \frac{E^{re}(i)}{\max\left[E^{re}_{N_2}(i)\right]}, \tag{16}$$

where ϕ_i is the normalized EF and $E^{re}_{N_2}(i)$ indicates the set of residual energy of the two-hop node i.

D. NSF

The node stability affects cluster lifetime. The main objective of NSF is to find the appropriate node that is close to CH as shown in Fig. 4. In our cluster model, we consider the node stability factor based on transmission power as follows:

$$NSF = \begin{cases} 1 - \dfrac{|d_{min} - d_{ij}|}{d_{min}}, & 0 \le d_{ij} < d_{min} \\ 1, \quad d_{min} \le d_{ij} \le d_{max} \\ 1 - \dfrac{|d_{min} - d_{max}|}{R - d_{max}}, & d_{max} \le d_{ij} \le 2R, \end{cases} \tag{17}$$

where d_{ij}, d_{min}, and d_{max} are the distance between node i and j, minimum transmission distance ($0 \le d_{min} < d_{max}$), and maximum transmission distance ($d_{min} < d_{max} \le R$), respectively.

Moreover, R, $2R$ are one-hop, two-hop communication distances. If the distance between two nodes i and j is d_{min} that means they are very close to each other resulting in higher NSF. On the other hand, if the distance is d_{max} then they are far away from each other, but still within a communication radius, as shown in Fig. 4.

E. CLUSTER FORMATION

The communication for WIoT is represented by a graph $G = (V, E)$, where V is the number of WIoT nodes and E is the set

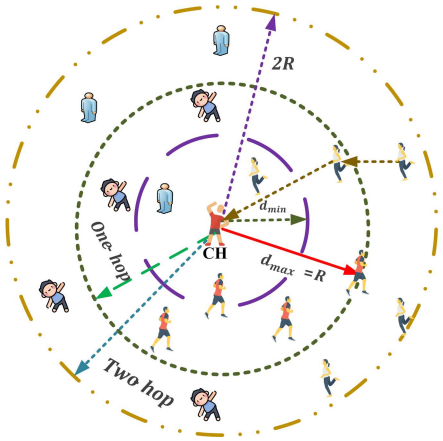

FIGURE 4. Illustration of NSF.

of links between WIoT nodes. For cluster formation based on TCR, EF, and NSF, we compute a weight factor W_i as follows:

$$W_i = \eta \times TCR + \theta \times EF + \xi \times NSF, \tag{18}$$

where η, θ, and ξ are the weight coefficients of the corresponding metrics and $\eta + \theta + \xi = 1$. Our proposed DECR algorithm is distributed where each node obtains the two-hop neighbor information. As we considered three critical parameters TCR, EF, and NSF during the clustering process, the DECR works in highly dynamic networks. The pseudo-code for the proposed clustering algorithm is described in Algorithm 1.

Algorithm 1 Cluster Formation of DECR

Input: Node information
Output: Cluster formation
Procedure
Initialize $N(i) = \emptyset$ and $W_i = 0$.
for *every node* $i \in V$ **do**
  Broadcast Hello packet (ID_i, TCR_i, EF_i, NSF_i);
  if *any node i received Hello packet* **do**
    $|N(i)| = |N(i)| + 1$;
    Update the TCR_i value by Equation (14);
    Node degree $Deg(i) = |N(i)|$;
    Update the CRL_i list;
  end if
  Update weight value W_i by Equation (18);
  Broadcast Hello packet;
  $N_1(i).add$ (One-hop neighbor node);
  $N_2(i).add$ (Two-hop neighbor node);
  $N_{1-2}(i) \Leftarrow N_1(i) \bigcup N_2(i)$
end for
end procedure

At the initial stage, each node exchanges the Hello packet, as shown in Fig. 3(a). After receiving the Hello packet, each node builds its neighbor table based on the connectivity ratio, which also gives us the degree of a node. Subsequently, each node builds a clustering record list (CRL) based on the degree of a node. In the second step, the weight factor is calculated by Equation (18), and again, each node broadcasts the Hello packet, as shown in Fig. 3(b). After receiving the Hello packet, Algorithm 1 completes the one- and two-hop neighbor node lists. Finally, after obtaining the one-hop and two-hop node information, the proposed algorithm forms a cluster, which includes one-hop and two-hop neighbor nodes.

F. OPTIMAL NUMBER OF CLUSTERS

Assume that the average number of clusters is C and the average number of nodes per cluster is $\frac{N}{C}$, where N is the number of nodes [44]. The number of CH per cluster is only one, therefore each cluster contains $\frac{N}{C} - 1$ number of the cluster member nodes. As we consider two-hop neighbors for clustering, the number of one-hop and two-hop nodes per cluster is calculated as follows

$$\mathrm{E}[N_1] = \frac{\pi R^2}{\pi (2R)^2} \cdot \left(\frac{N}{C} - 1\right). \tag{19}$$

$$\mathrm{E}[N_2] = \left(\frac{N}{C} - 1 - |N(i)|\right) = \frac{3}{4}\left(\frac{N}{C} - 1\right). \tag{20}$$

As intra-cluster distance is a key parameter, we consider the two-hop neighbor-based clustering. A two-hop neighbor-based cluster will be larger than a one-hop-based cluster. The average distance square between the CH node and two-hop neighbor nodes is expressed as

$$d(\mathrm{CH}, N_2) = \frac{M^2}{2\pi C}, \tag{21}$$

where M is the square area. The average distance square between the CH node and one-hop neighbor nodes is presented as

$$d(\mathrm{CH}, N_1) = \frac{M^2}{8\pi C}. \tag{22}$$

Therefore, the average distance square between one-hop neighbor nodes and two-hop neighbor nodes can be defined as

$$d(N_1, N_2) = \frac{M^2}{8\pi C}. \tag{23}$$

Two-hop neighbor nodes transmit the data to one-hop neighbor nodes. The energy consumption for this transmission is defined as

$$\begin{aligned} E_{\mathrm{Tx(2h,1h)}} &= N_2 \cdot E_{\mathrm{Tx}}(l, \Delta d) \\ &= \frac{3}{4}\left(\frac{N}{C} - 1\right) \cdot l \cdot \left(E_{\mathrm{elec}} + \varepsilon_{f_s} \cdot \frac{M^2}{8\pi C}\right). \end{aligned} \tag{24}$$

The energy consumption for receiving data from two-hop nodes to one-hop neighbor nodes is defined as

$$\begin{aligned} E_{\mathrm{Rx(2h,1h)}} &= N_1 \cdot 3 \cdot E_{\mathrm{Rx}}(l) \\ &= \frac{3}{4}\left(\frac{N}{C} - 1\right) \cdot l \cdot E_{\mathrm{elec}}. \end{aligned} \tag{25}$$

The energy consumption of transmitting aggregate data from the one-hop neighbor to the CH node is defined as

$$E_{\mathrm{Tx(1h,CH)}} = N_1 \cdot E_{\mathrm{Tx}}(l,d) = \frac{1}{4}\left(\frac{N}{C}-1\right)\cdot l \cdot \left(E_{\mathrm{elec}} + \varepsilon_{f_s}\cdot \frac{M^2}{8\pi C}\right). \quad (26)$$

The energy consumption of received aggregate data from the one-hop neighbor to the CH node is defined as

$$E_{\mathrm{Rx(1h,CH)}} = N_1 \cdot E_{\mathrm{Rx}}(l) = \frac{1}{4}\left(\frac{N}{C}-1\right)\cdot l \cdot E_{\mathrm{elec}}. \quad (27)$$

Therefore, total energy consumption for data transmission between two-hop neighbor nodes to CH node can be calculated as follows

$$E_{\mathrm{intra}} = E_{\mathrm{Tx(2h,1h)}} + E_{\mathrm{Rx(2h,1h)}} + E_{\mathrm{Tx(1h,CH)}} + E_{\mathrm{Rx(1h,CH)}}. \quad (28)$$

For the inter-cluster transmission, we used relay nodes to transmit the data to the sink, and energy consumption for relay inter-cluster data is defined as

$$E_{\mathrm{relay}} = E_{\mathrm{Rx}}(l) + E_{\mathrm{Tx}}(l,d). \quad (29)$$

The total energy consumption E_{total} of the entire network will be a summation of all intra-cluster and inter-cluster energy consumption. First derivation of E_{total} provides the optimal number of clusters as follows

$$\frac{dE_{\mathrm{total}}}{dC} = 0. \quad (30)$$

$$C_{\mathrm{opt}} = \left\{ C \mid C \in N, \frac{dE_{\mathrm{total}}}{dC} = 0 \right\}. \quad (31)$$

Finally, for the N number of nodes the optimal probability to become CH in the network is $\frac{C_{\mathrm{opt}}}{N}$.

G. CLUSTER HEAD SELECTION

For the CH selection, we utilized the MGWO algorithm. The CH selection process is described in Algorithm 2. As GWO algorithm offers the three best solutions alpha, beta, and delta according to the sequence. Therefore, the alpha node is the best solution with the best knowledge about the search space whose position is more likely to be near the prey. Initially, the CH is selected based on the node connectivity ratio and energy level. We formulated a fitness function based on TCR value and EF as follows:

$$F(CH_m) = \begin{cases} \lambda \cdot \dfrac{E^{re}(i)}{E^{int}(i)} + (1-\lambda)\cdot TCR_i, & E^{re}(i) > 0 \\ 0, & E^{re}(i) \le 0. \end{cases} \quad (32)$$

where λ is the weight coefficient of the corresponding fitness function. A node with higher residual energy and connectivity ratio will be selected as a CH. When the current alpha node energy level reaches the threshold level, the next CH may choose from the beta node. CH lifetime is obtained as follows

$$CH_m^{LT} = \frac{E^{re}(i)}{E_{\mathrm{total}}}, \quad (33)$$

where E_{total} indicates the total amount of energy consumption in a single round. Subsequently, the position of the prey is updated as follows

$$X_n^d(t+1) = F_{n,\alpha}X_{n,\alpha}^d(t+1) + F_{n,\beta}X_{n,\beta}^d(t+1) + F_{n,\delta}X_{n,\delta}^d(t+1), \quad (34)$$

$$F_{n,\alpha} = \frac{F_\alpha}{F_\alpha + F_\beta + F_\delta}, F_{n,\beta} = \frac{F_\beta}{F_\alpha + F_\beta + F_\delta}, F_{n,\delta} = \frac{F_\delta}{F_\alpha + F_\beta + F_\delta}, \quad (35)$$

where $F_{n,\alpha}$, $F_{n,\beta}$, and $F_{n,\delta}$ are the weight of the alpha, beta, and delta wolf respectively and F_α, F_β, and F_δ are the three best fitness values.

Algorithm 2 MGWO-Based CH Selection

Input: Clusters C_m and number of nodes N
Output: Cluster head CH_m, where $m = 1, 2, \ldots, ??$.
/* **Initialization phase** */
1: Initialize the position of the wolf pack $X = [X_1, \ldots, X_n, \ldots, X_N]$.
2: Initialize the MGWO parameters (a, A_n^d, C_n^d).
/* **Computation** */
3: **while** $(t < t_{max})$, **do**
4: **for** each search agent CH_m **do**
5: Compute the fitness value using Equation (32);
6: Select the three best solutions $X_{n,\alpha}^d$, $X_{n,\beta}^d$, and $X_{n,\delta}^d$;
7: Update the coefficient vector (a, A_n^d, C_n^d);
8: Update the wolf position using (8)–(12);
9: Update the prey position using (35);
10: **end for**
11: $t = t + 1$
12: **end while**
13: return CH_m

Initially, the positions of the wolf pack and the MGWO parameters are initialized in lines 1–2. For each round to select the CH from the wolf pack, a fitness value is computed based on Equation (32). According to the principle of the MGWO algorithm, we obtain the three best solutions by using Equations (8)–(12). Finally, the algorithm selects the alpha wolf as a CH.

H. ENERGY-EFFICIENT ROUTING

In this paper, routing is categorized in two ways. First, all the WIoT nodes transmit their data to the nearest CH node. Nodes placed at a two-hop distance from CH transmit their data to one-hop neighbor nodes, and then one-hop neighbor nodes transmit the received data to its nearest CH. Second, CH receives data and aggregates the data. After intra-cluster transmission, inter-cluster transmission happened. Details of

the process of intra-cluster transmission are described in the first part of Algorithm 3. To optimize the inter-cluster transmission, we utilized the MGWO algorithm. The proposed algorithm's objective is to choose the high residual nodes during routing to distribute energy over the whole network and minimize the transmission distance between the CH to the sink.

When the sink node is out of range from the CH nodes, the CH nodes utilized the multi-hop routing to transmit data to the sink. In the routing path, we choose high residual energy nodes as follows:

$$RP_{next-hop}(CH_i, CH_j) \propto E^{re}(CH_j), \tag{36}$$

where $RP_{next-hop}(CH_i, CH_j)$ is the next-hop routing between CH_i and CH_j. A CH needs to select its nearest CH for data transmission as follows

$$RP_{next-hop}(CH_i, CH_j) \propto \frac{1}{(CH_i - CH_j)}. \tag{37}$$

A CH requires to choose the next hop CH, who is nearest to the sink node as follows

$$RP_{next-hop}(CH_i, CH_j) \propto \frac{1}{(CH_j - sink)}. \tag{38}$$

Finally, the MGWO fitness value is computed for routing as follows

$$RP_{next-hop}(CH_i, CH_j) \propto \frac{E^{re}(CH_j)}{\|CH_i - CH_j\| \cdot \|CH_j - sink\|}. \tag{39}$$

$$Mini: F = RP_{next-hop}(CH_i, CH_j) \propto \frac{E^{re}(CH_j)}{\|CH_i - CH_j\| \cdot \|CH_j - sink\|}. \tag{40}$$

Inter-cluster routing is presented in Algorithm 3 second part.

Algorithm 3 MGWO-Based Routing

Input: Cluster formation, Cluster head CH_m, where $m = 1, 2, \ldots, \mathbb{M}$.
Output: Best routing path $RP_{next-hop}$
/* **Initialization** */
1: Position of the wolf pack $X = [X_1, \ldots, X_n, \ldots, X_N]$.
2: MGWO parameters (a, A_n^d, C_n^d) and $(X_\alpha^d, X_\beta^d, X_\delta^d)$.
3: Iteration $t = 1$ and allow maximum iteration number t_{max}.
/* **Intra-cluster routing** */
4: **for** all CMs $\in N_2(i) \backslash N_1(i) \cap CH$ **do**
5: Transmit data to the nearest CM $\in N_1(i) \backslash N_1(i) \cap CH$;
6: **end for**
7: **for** all CMs $\in N_1(i) \backslash N_1(i) \cap CH$ **do**
8: Received data from CM $\in N_2(i) \backslash N_2(i) \cap CH$;
9: Transmit data to the nearest CM $\in$ CH;
10: **end for**
/* **Inter-cluster routing** */
11:**for** all CM $\in$ CH **do**
12: Received data from CM and aggregate data;
13: **end for**
14: Compute the fitness value using Equation (40) for each search agent;
15: **for** $(t < t_{max})$, **do**
16: Update the position of the search agent by (8)–(12);
17: Update (a, A_n^d, C_n^d);
18: For each search agent, compute the fitness value by (36)–(39);
19: Select the three best solutions X_α^d, X_β^d, and X_δ^d;
20: **end for**
21: Return the best $RP_{next-hop}(\mathrm{CH}_i) = RP_{best}$

I. COMPUTATIONAL COMPLEXITY

In our network model, we consider N number of WIoT nodes. Every node is involved in the CH selection process by broadcasting the Hello packet. Therefore $O(n)$ number of packet broadcast for CH selection. After the CH selection, CH_m node broadcasts an announcement, where $O(m)$ number of packets broadcast. All the CMs need to compare the distance after getting the CH announcement. The total communication overhead for the clustering process is $O(mn)$. Moreover, each node broadcasts the Hello packet to its one-hop neighbor nodes; thus, the algorithm overhead for this process requires $O(n)$. We assume that the maximum number of iterations is t_{max}. The total communication overhead for the clustering process is $O(mn^2 t_{max})$.

To compute the overhead for routing we assume that h_{max} number of hops are required to send the data from CM to sink. Thus, the communication overhead for CH_m number of nodes is $O(mh_{max})$. In DECR, the total overhead is the combination of clustering and routing overhead, that is $O(mn^2 t_{max} + mh_{max})$.

V. PERFORMANCE EVALUATION

To evaluate the performance of the proposed DECR, we conducted an extensive computer simulation using MATLAB R2021a [45]. Moreover, we compared our proposed DECR with two recent clustering and routing protocols, MT-MAC [28] and ALOC [31]. Both ALOC and MT-MAC were designed for WBAN applications.

A. SIMULATION ENVIRONMENT

In our simulation, initially, 100 nodes are deployed in a 100m × 100m square region. All nodes are uniformly distributed in a random fashion. The sink node is placed at the center of the region with the coordinate of (50m, 50m) for scenario-1 and in the scenario-2 sink position is outside of the network area with the coordinate of (0m, 0m). All nodes have a random waypoint mobility (RWM) model, and the speed of nodes is 2 to 5 m/s [37]. Simulation parameters are summarized in Table 3.

We compared DECR with MT-MAC and ALOC in terms of the packet delivery ratio (PDR), control overhead (CO), average end-to-end (AE2E) delay, network lifetime, network energy consumption, cluster building time, and cluster

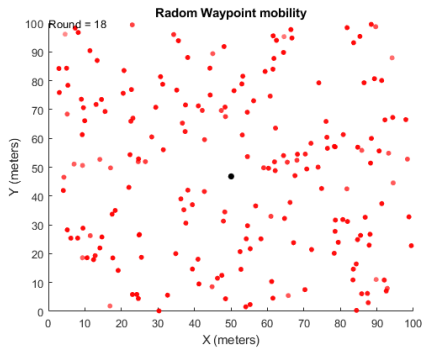

FIGURE 5. Deployment of WIoT nodes in an RWM model.

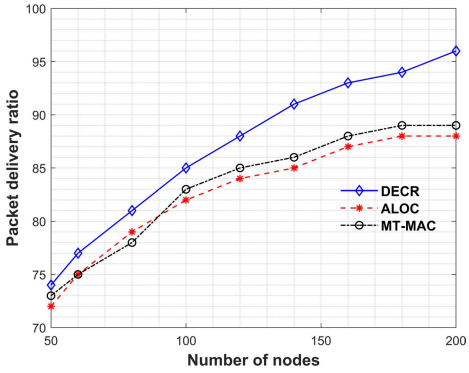

FIGURE 6. PDR vs. number of nodes.

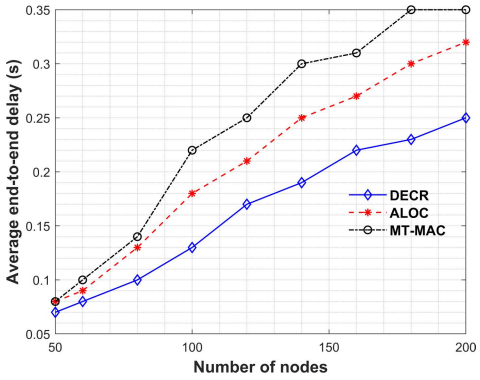

FIGURE 7. AE2E delay vs. number of nodes.

lifetime. The definition of the above performance metrics is defined in [21].

B. SIMULATION RESULTS AND DISCUSSION FOR SCENARIO-1

In this subsection, we analyzed and compared the performance of DECR algorithm with the existing clustering and routing protocol.

The simulation environment is presented in Fig. 5, where 200 nodes are deployed randomly and uniformly distributed on a 100 m^2 square region.

The sink node indicated by the black color is located at the center of the region. All the nodes can move freely and follow the RWM model, which is more similar to the human walk.

1) PDR VS. NUMBER OF NODES

As depicted in Fig. 6, we investigated the performance of protocols by varying node densities in the network. Herein, we varied the nodes from 50 to 200. Node densities have an impact on PDR. Because of the low density, the nodes face frequent link disconnection problems resulting in low PDR. After increasing the number of nodes, PDR increases sharply for all the protocols. However, our proposed DECR performs better than MT-MAC and ALOC. This is because we considered the two-hop neighbor-based clustering that works better than the one-hop neighbor-based clustering. Two-hop neighbor information extends the overall network knowledge and reduces packet loss even in high node mobility. Moreover, when the number of nodes is less, the number of CH is also less; thus, CM nodes need to transmit data to the CH from a distance. However, after increasing the number of nodes, the number of CH increases as many, resulting in higher PDR.

2) AE2E DELAY VS. NUMBER OF NODES

As depicted in Fig. 7, as the node density increases, AE2E delay also increases. This is because it takes time to find the node position and route building time when the nodes are mobile. Our two-hop neighbor scheme minimizes the node AE2E delay compared to the one-hop-based clustering and routing protocols. In DECR, we utilized a new factor called NSF in clustering, which provides cluster stability.

3) CO VS. NUMBER OF NODES

Fig. 8 presents the effect of CO as a function of node densities. CO is one of the critical factors in low-energy networks like WBANs, measuring the Hello packet exchange for clustering and CH selection. Initially, DECR showed higher CO compared to ALOC. Generally, two-hop neighbor information utilized more CO than the one-hop neighbor-based clustering protocol. However, in our case, our proposed protocol is more stable in clustering than ALOC and MT-MAC, which significantly increase the cluster lifetime, thus reducing the re-clustering.

4) CLUSTER BUILDING TIME VS. NUMBER OF NODES

The cluster building time refers to the cluster formation and CH selection time. Long cluster setup time indicates the protocol complexity is high. Fig. 9 illustrates that node densities impact the clustering building time. In our DECR, we used MGWO for CH selection. Like other bio-inspired algorithms, we utilized a fitness value to select the CH. The MGWO computational complexity is significantly low compared to other bio-inspired algorithms. Concerning a large number of nodes, the cluster-building time increases significantly for most of the clustering protocols. However, in DECR,

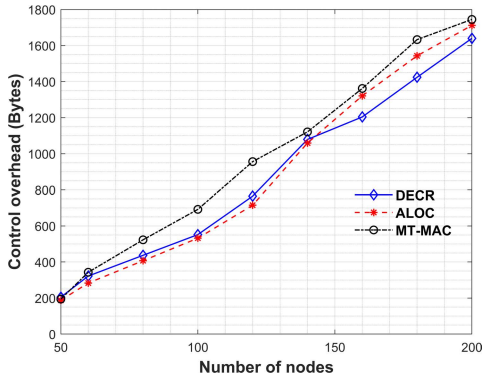

FIGURE 8. CO vs. number of nodes.

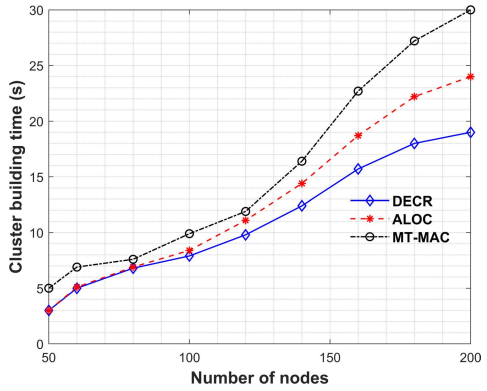

FIGURE 9. Cluster building time vs. number of nodes.

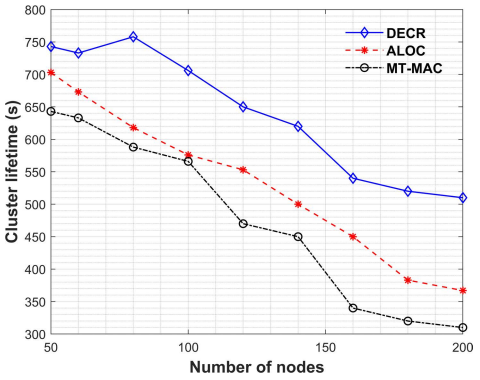

FIGURE 10. Cluster lifetime vs. number of nodes.

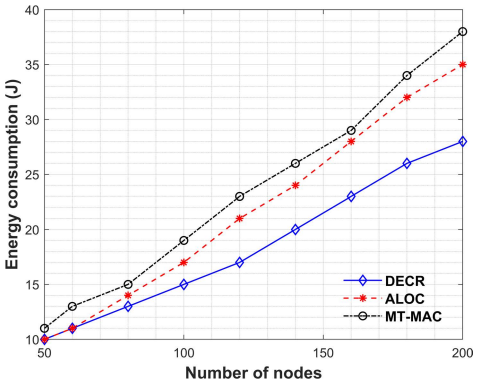

FIGURE 11. Energy consumption vs. number of nodes.

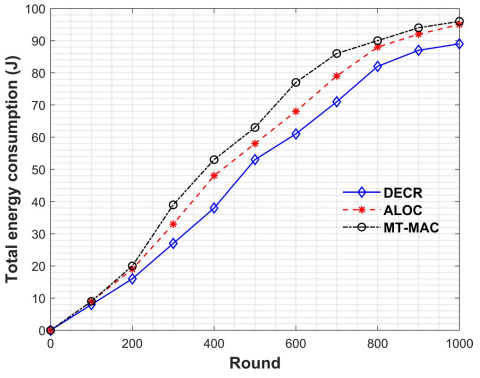

FIGURE 12. Total energy consumption vs. round.

we utilized our designed Hello packet and the TCR factor reduced our clustering building time.

5) CLUSTER LIFETIME VS. NUMBER OF NODES

The time from a cluster formation to its destruction indicates the cluster lifetime, which is an important factor for network energy consumption. In DECR, a node with a higher fitness value takes over the position of CH. In our proposed work, we consider TCR and residual energy as key fitness values for CH selection.

We defined the cluster lifetime in Equation (33). When the node energy goes down from a certain threshold level, the algorithm needs to activate the CH selection process since a short cluster lifetime increases the CO because of re-clustering and CH selection. Fig. 10 depicts that the cluster lifetime decreases as node densities increase. Due to the node mobility, the network topology frequently changes, resulting in a lower cluster lifetime.

6) ENERGY CONSUMPTION VS. NUMBER OF NODES

Fig. 11 illustrates that the energy consumption varies as the node density changes. The DECR consumes less energy than ALOC and MT-MAC because it considers node energy as a crucial factor in clustering, CH selection, and routing due to the optimal number of clusters. In our proposed approach, we analytically optimize the number of clusters for our network, which minimizes the number of single-node clusters resulting in low energy consumption.

7) TOTAL ENERGY CONSUMPTION VS. ROUND

Since WBANs are mostly run by limited battery power, energy consumption is the key factor in evaluating the performance of clustering and routing protocol. Fig 12 depicts the total energy consumption as a function of rounds.

From Fig. 12, it can be observed that MT-MAC consumes more energy than ALOC and DECR. DECR's overall energy consumption curve is slow and stable mainly due to two-hop

TABLE 4. Performance metrics comparison for different Simulation scenarios.

Parameter	Protocols	PDR	Total raw packets to sink	AE2E (s)	FND	HND	AND	Average network energy consumption rate
Scenario-1	DECR	96%	43095	0.25	178	461	982	0.0882 J/round
	ALOC	88%	37465	0.32	96	396	848	0.0971 J/round
	MT-MAC	89%	38129	0.35	95	375	798	0.0962 J/round
Scenario-2	DECR	93%	40212	0.31	154	398	928	0.0897 J/round
	ALOC	84%	35332	0.45	90	336	758	0.0991 J/round
	MT-MAC	82%	33312	0.54	85	315	716	0.1162 J/round

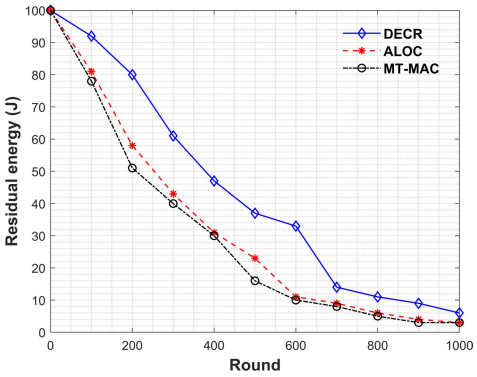

FIGURE 13. Residual energy vs. round.

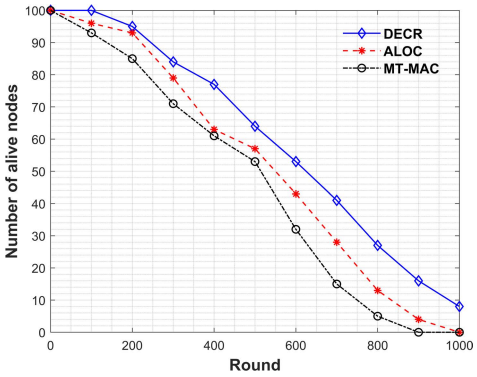

FIGURE 14. Number of living nodes vs. round.

clustering, the optimal number of CH, and energy-efficient routing. Utilizing two-hop neighbor information in clustering helps the two-hop nodes transmit the data to the CH node by using one-hop neighbor nodes as a relay node. This process reduces the energy consumption in receiving the data from long-distance nodes.

8) RESIDUAL ENERGY VS. ROUNDS

Fig. 13 represents the rate of the node residual energy decrease. The proposed DECR has higher residual energy than ALOC and MT-MAC since the DECR protocol distributes the energy consumption between the nodes, which makes the death node slower. Therefore, in DECR, more nodes can survive compared with other methods.

9) NUMBER OF LIVING NODES VS. ROUNDS

In our simulation, we consider a node as a dead node when it drains its battery completely. Fig. 14 represents the number of alive nodes for a round. DECR balances the energy consumption between the nodes, resulting in a slower node death rate. Our proposed approach balances the network topology well by better clustering, optimizing the number of CH, balancing the transmission distance into the cluster, and reducing the inter-cluster transmission distance, leading to less energy consumption in the network. Low energy consumption, higher residual energy, and a higher number of living nodes indicate the protocol stability.

C. SIMULATION RESULTS AND DISCUSSION FOR SCENARIO-2

In scenario-2, 200 nodes are deployed randomly and uniformly distributed on a 200 m^2 square region and a sink node is placed outside of the network area. Here, DECR has been simulated for evaluating the PDR, AE2E delay, the total number of raw packets to sink, and average network energy consumption rate in scenario-1 and 2. Additionally, the simulation results of the round of first node death (FND), half node death (HND), and all node death (AND) are presented and their outcomes have been compared with existing clustering algorithms in Table 4.

We found that the proposed algorithm extends the network lifetime, and this happens because of the inclusion of energy-efficient clustering, CH selection, and packet routing strategy. The number of raw packets sent to the sink node can well represent the transmission efficiency of the routing protocol. For both scenarios, DECR shows higher FND, HND, and AND compared with ALOC and MT-MAC. Results show that when the sink is placed outside of the network area, shorter is the life span of WIoT nodes. The amount of data is spectacular when the sink is located at the center of the network.

VI. CONCLUSION

In this paper, we have proposed a distributed energy-efficient clustering and routing protocol for WIoT-enabled WBANs. The proposed DECR has three phases: cluster formation, CH selection, and routing. For the cluster formation,

we utilized two-hop neighbor information. Two-hop neighbor information extends the local view of the network topology, which helps maintain the network topology. Moreover, we also introduce new factors such as TCR, EF, and NSF, which are jointly considered for cluster formation. In the CH selection phase, we utilized the MGWO algorithms inspired by GWO. The node TCR and residual energy are considered to select the CH node. Our proposed analytical model helps compute the optimal number of clusters in the network. Finally, our energy-efficient routing optimizes intra- and inter-cluster communication. The simulation results indicate that the proposed DECR is superior in performance metrics such as PDR, AE2E delay, control overhead, cluster building time, cluster lifetime, and network energy consumption. Additionally, the distributed energy balancing among the nodes significantly prolongs the overall network lifetime.

In our future work, we will consider finding more optimal solutions using different heuristic algorithms.

ACKNOWLEDGMENT

The authors would like to thank the editor and anonymous referees for their constructive comments for improving the quality of this paper.

REFERENCES

[1] B. Xiao, H. Wong, D. Wu, and K. L. Yeung, "Design of small multiband full-screen smartwatch antenna for IoT applications," *IEEE Internet Things J.*, vol. 8, no. 24, pp. 17724–17733, Dec. 2021, doi: 10.1109/jiot.2021.3082535.

[2] (2022). *Statistics Korea*. Accessed: Jan. 1, 2022. [Online]. Available: http://kostat.go.kr

[3] J. Mu, Y. Wei, H. Ma, and Y. Li, "Spectrum allocation scheme for intelligent partition based on machine learning for inter-WBAN interference," *IEEE Wireless Commun.*, vol. 27, no. 5, pp. 32–37, Oct. 2020, doi: 10.1109/mwc.001.1900551.

[4] M. Y. Arafat and S. Moh, "JRCS: Joint routing and charging strategy for logistics drones," *IEEE Internet Things J.*, vol. 9, no. 21, pp. 21751–21764, Nov. 2022, doi: 10.1109/JIOT.2022.3182750.

[5] L. Zhong, S. He, J. Lin, J. Wu, X. Li, Y. Pang, and Z. Li, "Technological requirements and challenges in wireless body area networks for health monitoring: A comprehensive survey," *Sensors*, vol. 22, no. 9, p. 3539, May 2022, doi: 10.3390/s22093539.

[6] M. Aledhari, R. Razzak, B. Qolomany, A. Al-Fuqaha, and F. Saeed, "Biomedical IoT: Enabling technologies, architectural elements, challenges, and future directions," *IEEE Access*, vol. 10, pp. 31306–31339, 2022, doi: 10.1109/access.2022.3159235.

[7] F. John Dian, R. Vahidnia, and A. Rahmati, "Wearables and the Internet of Things (IoT), applications, opportunities, and challenges: A survey," *IEEE Access*, vol. 8, pp. 69200–69211, 2020, doi: 10.1109/access.2020.2986329.

[8] M. Salayma, A. Al-Dubai, I. Romdhani, and Y. Nasser, "Wireless body area network (WBAN)," *ACM Comput. Surv.*, vol. 50, no. 1, pp. 1–38, Jan. 2018, doi: 10.1145/3041956.

[9] A. Arghavani, H. Zhang, Z. Huang, Y. Chen, and Z. Chen, "Tuatara: Location-driven power-adaptive communication for wireless body area networks," *IEEE Trans. Mobile Comput.*, vol. 22, no. 1, pp. 574–588, Jan. 2023, doi: 10.1109/tmc.2021.3070296.

[10] Y. Qu, G. Zheng, H. Ma, X. Wang, B. Ji, and H. Wu, "A survey of routing protocols in WBAN for healthcare applications," *Sensors*, vol. 19, no. 7, p. 1638, 2019, doi: 10.3390/s19071638.

[11] G. Newell and G. Vejarano, "Motion-based routing and transmission power control in wireless body area networks," *IEEE Open J. Commun. Soc.*, vol. 1, pp. 444–461, 2020, doi: 10.1109/ojcoms.2020.2986396.

[12] Y. Gong and G. Lai, "Low-energy clustering protocol for query-based wireless sensor networks," *IEEE Sensors J.*, vol. 22, no. 9, pp. 9135–9145, May 2022, doi: 10.1109/jsen.2022.3159546.

[13] Z. Ullah, I. Ahmed, K. Razzaq, M. K. Naseer, and N. Ahmed, "DSCB: Dual sink approach using clustering in body area network," *Peer-Peer Netw. Appl.*, vol. 12, no. 2, pp. 357–370, 2017, doi: 10.1007/s12083-017-0587-z.

[14] N. Samarji and M. Salamah, "ERQTM: Energy-efficient routing and QoS-supported traffic management scheme for SDWBANs," *IEEE Sensors J.*, vol. 21, no. 14, pp. 16328–16339, Jul. 2021, doi: 10.1109/jsen.2021.3075241.

[15] R. Hamidouche, Z. Aliouat, A. A. A. Ari, and M. Gueroui, "An efficient clustering strategy avoiding buffer overflow in IoT sensors: A bio-inspired based approach," *IEEE Access*, vol. 7, pp. 156733–156751, 2019, doi: 10.1109/access.2019.2943546.

[16] M. Y. Arafat and S. Moh, "Localization and clustering based on swarm intelligence in UAV networks for emergency communications," *IEEE Internet Things J.*, vol. 6, no. 5, pp. 8958–8976, Oct. 2019, doi: 10.1109/jiot.2019.2925567.

[17] Y. Liu, C. Li, J. Xiao, Z. Li, W. Chen, X. Qu, and J. Zhou, "QEGWO: Energy-efficient clustering approach for industrial wireless sensor networks using quantum-related bioinspired optimization," *IEEE Internet Things J.*, vol. 9, no. 23, pp. 23691–23704, Dec. 2022, doi: 10.1109/JIOT.2022.3189807.

[18] S. M. Bozorgi, M. R. Hajiabadi, A. A. R. Hosseinabadi, and A. K. Sangaiah, "Clustering based on whale optimization algorithm for IoT over wireless nodes," *Soft Comput.*, vol. 25, no. 7, pp. 5663–5682, Apr. 2021, doi: 10.1007/s00500-020-05563-7.

[19] P. Ekler, J. Levendovszky, and D. Pasztor, "Energy aware IoT routing algorithms in smart city environment," *IEEE Access*, vol. 10, pp. 87733–87744, 2022, doi: 10.1109/access.2022.3199757.

[20] O. Alzamzami and I. Mahgoub, "Link utility aware geographic routing for urban VANETs using two-hop neighbor information," *Ad Hoc Netw.*, vol. 106, Sep. 2020, Art. no. 102213, doi: 10.1016/j.adhoc.2020.102213.

[21] M. Y. Arafat and S. Moh, "A Q-learning-based topology-aware routing protocol for flying ad hoc networks," *IEEE Internet Things J.*, vol. 9, no. 3, pp. 1985–2000, Feb. 2021, doi: 10.1109/JIOT.2021.3089759.

[22] J. Mu, R. Stewart, L. Han, and D. Crawford, "A self-organized dynamic clustering method and its multiple access mechanism for multiple WBANs," *IEEE Internet Things J.*, vol. 6, no. 4, pp. 6042–6051, Aug. 2019, doi: 10.1109/jiot.2018.2869829.

[23] J. Park, "Bio-inspired approach for inter-WBAN coexistence," *IEEE Trans. Veh. Technol.*, vol. 68, no. 7, pp. 7236–7240, Jul. 2019, doi: 10.1109/tvt.2019.2917915.

[24] P.-Y. Kong, "Cellular-assisted device-to-device communications for healthcare monitoring wireless body area networks," *IEEE Sensors J.*, vol. 20, no. 21, pp. 13139–13149, Nov. 2020, doi: 10.1109/jsen.2020.3001727.

[25] S. M. Shimly, D. B. Smith, and S. Movassaghi, "Experimental analysis of cross-layer optimization for distributed wireless body-to-body networks," *IEEE Sensors J.*, vol. 19, no. 24, pp. 12494–12509, Dec. 2019, doi: 10.1109/jsen.2019.2937356.

[26] Z. Ullah, I. Ahmed, F. A. Khan, M. Asif, M. Nawaz, T. Ali, M. Khalid, and F. Niaz, "Energy-efficient harvested-aware clustering and cooperative routing protocol for WBAN (E-HARP)," *IEEE Access*, vol. 7, pp. 100036–100050, 2019, doi: 10.1109/access.2019.2930652.

[27] D. Olivia, A. Nayak, and M. Balachandra, "Data-centric load and QoS-aware body-to-body network routing protocol for mass casualty incident," *IEEE Access*, vol. 9, pp. 70683–70699, 2021, doi: 10.1109/access.2021.3077472.

[28] A. Zeb, S. Wakeel, T. Rahman, I. Khan, M. I. Uddin, and B. Niazi, "Energy-efficient cluster formation in IoT-enabled wireless body area network," *Comput. Intell. Neurosci.*, vol. 2022, pp. 1–11, Apr. 2022, doi: 10.1155/2022/2558590.

[29] X. Li, J. Cai, J. Yang, L. Guo, S. Huang, and Y. Yi, "Performance analysis of delay distribution and packet loss ratio for body-to-body networks," *IEEE Internet Things J.*, vol. 8, no. 22, pp. 16598–16612, Nov. 2021, doi: 10.1109/jiot.2021.3075578.

[30] A. Sundar Raj and M. Chinnadurai, "Energy efficient routing algorithm in wireless body area networks for smart wearable patches," *Comput. Commun.*, vol. 153, pp. 85–94, Mar. 2020, doi: 10.1016/j.comcom.2020.01.069.

[31] F. Saleem, M. N. Majeed, J. Iqbal, A. Waheed, A. Rauf, M. Zareei, and E. M. Mohamed, "Ant lion optimizer based clustering algorithm for wireless body area networks in livestock industry," *IEEE Access*, vol. 9, pp. 114495–114513, 2021, doi: 10.1109/access.2021.3104643.

[32] M. D. Khan, Z. Ullah, A. Ahmad, B. Hayat, A. Almogren, K. H. Kim, M. Ilyas, and M. Ali, "Energy harvested and cooperative enabled efficient routing protocol (EHCRP) for IoT-WBAN," *Sensors*, vol. 20, no. 21, p. 6267, Nov. 2020, doi: 10.3390/s20216267.
[33] Y. Chang, H. Tang, Y. Cheng, Q. Zhao, B. Li, and X. Yuan, "Dynamic hierarchical energy-efficient method based on combinatorial optimization for wireless sensor networks," *Sensors*, vol. 17, no. 7, p. 1665, 2017, doi: 10.3390/s17071665.
[34] Z. Fei, B. Li, S. Yang, C. Xing, H. Chen, and L. Hanzo, "A survey of multi-objective optimization in wireless sensor networks: Metrics, algorithms, and open problems," *IEEE Commun. Surveys Tuts.*, vol. 19, no. 1, pp. 550–586, 1st Quart., 2017, doi: 10.1109/COMST.2016.2610578.
[35] Y. Chang, X. Yuan, B. Li, D. Niyato, and N. Al-Dhahir, "A joint unsupervised learning and genetic algorithm approach for topology control in energy-efficient ultra-dense wireless sensor networks," *IEEE Commun. Let.*, vol. 22, no. 11, pp. 2370–2373, Nov. 2018, doi: 10.1109/LCOMM.2018.2870886.
[36] Y. Chang, X. Yuan, B. Li, D. Niyato, and N. Al-Dhahir, "Machine-learning-based parallel genetic algorithms for multi-objective optimization in ultra-reliable low-latency WSNs," *IEEE Access*, vol. 7, pp. 4913–4926, 2019, doi: 10.1109/ACCESS.2018.2885934.
[37] J. Kim, N. Colabianchi, J. Wensman, and D. H. Gates, "Wearable sensors quantify mobility in people with lower limb amputation during daily life," *IEEE Trans. Neural Syst. Rehabil. Eng.*, vol. 28, no. 6, pp. 1282–1291, Jun. 2020, doi: 10.1109/tnsre.2020.2990824.
[38] S. Mirjalili, S. M. Mirjalili, and A. Lewis, "Grey wolf optimizer," *Adv. Eng. Softw.*, vol. 69, pp. 46–61, Mar. 2014, doi: 10.1016/j.advengsoft.2013.12.007.
[39] K. Luo, "Enhanced grey wolf optimizer with a model for dynamically estimating the location of the prey," *Appl. Soft Comput.*, vol. 77, pp. 225–235, Apr. 2019, doi: 10.1016/j.asoc.2019.01.025.
[40] X. Zhao, S. Ren, H. Quan, and Q. Gao, "Routing protocol for heterogeneous wireless sensor networks based on a modified grey wolf optimizer," *Sensors*, vol. 20, no. 3, p. 820, Feb. 2020, doi: 10.3390/s20030820.
[41] M. Y. Arafat and S. Moh, "Bio-inspired approaches for energy-efficient localization and clustering in UAV networks for monitoring wildfires in remote areas," *IEEE Access*, vol. 9, pp. 18649–18669, 2021, doi: 10.1109/ACCESS.2021.3053605.
[42] M. Fahad, F. Aadil, S. Khan, P. A. Shah, K. Muhammad, J. Lloret, H. Wang, J. W. Lee, and I. Mehmood, "Grey wolf optimization based clustering algorithm for vehicular ad-hoc networks," *Comput. Electr. Eng.*, vol. 70, pp. 853–870, Aug. 2018, doi: 10.1016/j.compeleceng.2018.01.002.
[43] M. S. Batta, H. Mabed, Z. Aliouat, and S. Harous, "A distributed multi-hop intra-clustering approach based on neighbors two-hop connectivity for IoT networks," *Sensors*, vol. 21, no. 3, p. 873, Jan. 2021, doi: 10.3390/s21030873.
[44] C. Chen, L.-C. Wang, and C.-M. Yu, "D2CRP: A novel distributed 2-hop cluster routing protocol for wireless sensor networks," *IEEE Internet Things J.*, vol. 9, no. 20, pp. 19575–19588, Oct. 2022, doi: 10.1109/jiot.2022.3148106.
[45] (2022). *MathWorks—Makers of MATLAB and Simulink*. Accessed: Jan. 11, 2022. [Online]. Available: https://www.mathworks.com

MUHAMMAD YEASIR ARAFAT received the B.Sc. degree in electronics and telecommunication engineering and the M.Sc. degree in computer networks and communication from Independent University, Bangladesh, in 2011 and 2014, respectively, and the Ph.D. degree in computer engineering from Chosun University, South Korea, in 2020. From 2011 to 2016, he worked at Amber IT Ltd., Bangladesh, as a Systems Manager. Since 2017, he has been a member of the Mobile Computing Laboratory, Chosun University, where he has been an Assistant Professor at the Department of Computer Engineering, since November 2020. He was a Korean Government Scholarship Program (KGSP) grantee and received the Minister Award from the Ministry of Education, South Korea, for his excellent study. His current research interests include ad hoc networks, unmanned aerial vehicle networks, and cognitive radio sensor networks with a focus on network architectures and protocols.

SUNGBUM PAN (Member, IEEE) received the B.S., M.S., and Ph.D. degrees in electronics engineering from Sogang University, South Korea, in 1991, 1995, and 1999, respectively. He was a Team Leader with the Biometric Technology Research Team, ETRI, from 1999 to 2005. He is currently a Professor with Chosun University. His current research interests include biometrics, security, and VLSI architectures for real time image processing.

EUNSANG BAK received the B.S. and M.S. degrees from Sogang University, Seoul, South Korea, and the Ph.D. degree from the University of North Carolina at Charlotte, in 2004. From 2004 to 2015, he worked as a Senior Research Engineer at Samsung Electronics Company Ltd., Suwon, South Korea. Since then, he has been a Research Professor at Chosun University, Gwangju, South Korea. His research interests include machine learning/pattern recognition, image processing, bioinformatics, and body area networks.